high-temperature–induced aggregation at the standard DSC concentrations.)

19. The COOH-terminal dansyl-lysine is placed at the end of the second α helix of BBL. Therefore, in the completely folded structure, the dansyl moiety is in relative proximity to the side chain of Lys_{36} (Fig. 1). In principle, in this configuration the intrinsic quantum yield of dansyl could be quenched by a proton transfer reaction from the protonated ε-amino group of Lys_{36}. Furthermore, the structure of BBL reveals a partially solvent-exposed hydrophobic core formed by inefficient packing between the two helices. A dansyl group hanging from a partially unfolded COOH-terminal tail can experience transient interactions with this core that will increase its quantum yield by effectively decreasing the average polarizability of its environment. These transient interactions between the dansyl group and the protein are sufficient to perturb its fluorescence quantum yield but do not substantially modify the energetics of BBL's unfolding (18).

20. M. M. Garcia-Mira, B. Ibarra-Molero, J. M. Sanchez-Ruiz, V. Muñoz, in preparation.

21. B. A. Schulman, P. S. Kim, C. M. Dobson, C. Redfield, Nature Struct. Biol. 4, 630 (1997).

22. A. K. Chamberlain, S. Marqusee, Biochemistry 37, 1736 (1998).

23. The 1D H^1 NMR spectrum of BBL at 293 K is well resolved and has large signal dispersion in the amide region [7.3 to 9.1 parts per million (ppm)], signaling a protein with defined 3D structure (fig. S1A). The 2D H^1 NMR analysis confirms this conclusion. Double-quantum filtered correlation, total correlation, and nuclear Overhauser effect (NOE) spectroscopy experiments produce 2D spectra with sharp cross peaks and little spectral overlap (fig. S1, B through E). All expected H^1 signals have been identified and assigned with the standard sequential procedure. The chemical shifts measured in our BBL construct coincide with those previously reported in a longer variant for which the high-resolution 3D structure has been determined (14). Differences in chemical shifts >0.1 ppm are only found for residues with ionizable groups or their sequence neighbors. These are most likely due to small pH discrepancies between the two experiments. Series of sequential NH–NH (i,i + 1) NOEs are clearly observed for residues in the NH_2- and COOH-terminal regions, indicating that the expected α helices are present (fig. S1D). Hδ-Hδ long-range NOEs that correspond to specific tertiary contacts in the native structure are also clearly observed (fig. S1E).

24. The model applied in this work is very similar to the one described previously by Muñoz & Eaton (32). The main statistical difference lies in the use of residues, instead of peptide bonds, as conformational units. The partition function has been truncated according to the single sequence approximation, as previously described (33). Under this approximation, the number of species in the model reduces to the total number of single stretches of native structure plus the random coil. Each species in the model is identified by two parameters: the position in the sequence of the first native residue and the number of residues in the native stretch [such as (1,40) for the fully native structure]. This approximation is quite accurate for calculating thermodynamic properties.

25. V. Muñoz, Curr. Opin. Struct. Biol. 11, 212 (2001).

26. V. Muñoz, W. A. Eaton, Proc. Natl. Acad. Sci. U.S.A. 96, 11311 (1999).

27. M. Sadqi, V. Muñoz, unpublished data.

28. S. Spector et al., J. Mol. Biol. 276, 479 (1998).

29. S. Spector, D. P. Raleigh, J. Mol. Biol. 293, 763 (1999).

30. S. J. Hagen, J. Hofrichter, A. Szabo, W. A. Eaton, Proc. Natl. Acad. Sci. U.S.A. 93, 11615 (1996).

31. M. V. Milburn et al., Science 247, 939 (1990).

32. M. Perutz, Nature 228, 726 (1970).

33. M. Young, K. Kirshenbaum, K. A. Dill, S. Highsmith, Protein Sci. 8, 1752 (1999).

34. E. Freire, Proc. Nat. Acad. Sci. U.S.A. 97, 11680 (2000).

35. Whatif for Windows, G. Vriend, J. Mol. Graph. 8, 52 (1990).

36. We thank B. Ibarra-Molero for collaborating in the data analysis and G. Lorimer for helpful suggestions on the

Evidence for Antibody-Catalyzed Ozone Formation in Bacterial Killing and Inflammation

Paul Wentworth Jr.,[1] Jonathan E. McDunn,[1]
Anita D. Wentworth,[1] Cindy Takeuchi,[2] Jorge Nieva,[3]
Teresa Jones,[1] Cristina Bautista,[1] Julie M. Ruedi,[3]
Abel Gutierrez,[3] Kim D. Janda,[1] Bernard M. Babior,[3]
Albert Eschenmoser[1,4] Richard A. Lerner[1]

Recently, we showed that antibodies catalyze the generation of hydrogen peroxide (H_2O_2) from singlet molecular oxygen ($^1O_2*$) and water. Here, we show that this process can lead to efficient killing of bacteria, regardless of the antigen specificity of the antibody. H_2O_2 production by antibodies alone was found to be not sufficient for bacterial killing. Our studies suggested that the antibody-catalyzed water-oxidation pathway produced an additional molecular species with a chemical signature similar to that of ozone. This species is also generated during the oxidative burst of activated human neutrophils and during inflammation. These observations suggest that alternative pathways may exist for biological killing of bacteria that are mediated by potent oxidants previously unknown to biology.

A central concept of immunology is that antibodies perform the sole function of marking antigens for destruction by effector systems such as complement and phagocytic cells (1). Work on antibody catalysis has demonstrated that the antibody molecule is capable of carrying out highly sophisticated chemistry, although there has been no direct evidence that this catalytic potential is used in nature (2). This view is consistent with the known organization of the humoral immune system, in that simple antigen binding is sufficient to activate more sophisticated effector systems and, thus, killing of pathogens can be achieved without the need to invoke any chemistry within the antibody molecule itself. Recently however, we found that all antibodies, regardless of source or antigenic specificity, can catalyze redox chemistry that is independent of antibody binding (3) and appears to be highly analogous to that carried out by the effector mechanism of phagocytic cells (4). When exposed to singlet molecular

oxygen ($^1O_2*$), antibodies oxidize water to produce H_2O_2 via the postulated intermediacy of H_2O_3 (5). In the present study, we examined whether this pathway might play any role in immune protective function of antibodies against bacteria and in inflammation.

Initial bactericidal studies focused on the gram-negative bacteria Escherichia coli (XL1-blue and O-112a,c) (6). Given the known bactericidal action of $^1O_2*$ itself (7), these studies required a $^1O_2*$ generating system that would not, on its own, kill E. coli (8) but would activate the water-oxidation pathway of antibodies. Negligible bactericidal activity against the two E. coli serotypes ($\sim 10^7$ cells/ml) was observed when hematoporphyrin IX (HPIX, 40 μM), an efficient sensitizer of $^3O_2$ (9), was irradiated with white light (light flux 2.7 mW cm^{-2}) for 1 hour in phosphate buffered saline (PBS, pH 7.4) at 4° ± 1°C. However, addition of antigen-specific or nonspecific monoclonal antibodies (20 μM) to this system resulted in killing of >95% of the bacteria (Fig. 1A) (6). This bactericidal action seems to be a general property of antibodies, in that regardless of origin or antigen specificity, all antibodies display this activity. This bactericidal activity was a function of antibody concentration (Fig. 1B), irradiation time (Fig. 1C), and HPIX concentration (at a given light flux) (Fig. 1D). These obser-

[1]Department of Chemistry, [2]Department of Immunology, [3]Department of Molecular and Experimental Medicine and The Skaggs Institute for Chemical Biology, The Scripps Research Institute, 10550 North Torrey Pines Road, La Jolla, CA 92037, USA. [4]Laboratorium für organische Chemie, Eidgenössichsche Technische Hochschule (ETH) Hönggerberg HCI-H309, Universitaetstrasse 16 CH-8093 Zürich, Switzerland.

Fig. 1. Killing of bacteria by antibodies. (**A**) Bar graph showing survival of *E. coli* XL1-blue and O112a,c strains [reported as percent recovered colony forming units (CFUs) at the start of the experiment ($t = 0$ min)]. Black and light gray bars correspond to the same experimental conditions, except that the light gray groups (2, 4, 6, 8, 10, and 12) were exposed to visible light for 60 min, whereas the black groups (1, 3, 5, 7, 9, and 11) were placed in the dark for 60 min. The bacterial cell density was ~ 10^7 cells/ml. Each data point is reported as the mean ± S.E.M. ($n = 6$) of *E. coli* XL1-blue (groups 1 to 6) and O112a,c (groups 7 to 12) are as follows, in PBS at 4°C. Groups 1 and –2: XL1-blue cells. Groups 3 and 4: HPIX, XL1-blue cells . Groups 5 and 6: XL1-blue–specific monoclonal antibody (25D11, 20 μM), HPIX, XL1-blue cells. Groups 7 and 8: O112a,c cells. Groups 9 and 10: HPIX, O112a,c cells. Groups 11 and 12: O112a,c-specific monoclonal antibody (15404; 20 μM), HPIX, O112a,c cells. (**B**) Concentration effect of O112a,c-specific monoclonal antibody, 15404, on the survival of *E. coli* O112a,c. Each data point is reported as the mean value ± S.E.M ($n = 3$). The [15404] that corresponds to killing of 50% of the cells (EC_{50}) = 81 ± 6 nM (**C**) Effect of irradiation time on the bactericidal action of *E. coli* XL1-blue–specific murine monoclonal antibody 12B2. Graph of irradiation time (2.7 mW cm^{-2}) versus survival of *E. coli* XL1-blue in the presence of HPIX and 12B2 (20 μM). Each data point is reported as the mean value ± S.E.M ($n = 3$). The time of irradiation that corresponds to killing of 50% of the cells = 30 ± 2 min (**D**) [HPIX]-dependence of *E. coli* XL1-blue-specific murine monoclonal antibody 25D11 bactericidal action. Graph of survival of *E.coli* XL1-blue versus exposure to a range of HPIX concentrations in PBS at 4°C under the following conditions. (■), XL1-blue cells in the dark, 60 min. (▲), XL1-blue cells in white light. (△), 25D11 (20 μM), XL1-blue cells in the dark, 60 min. (◆), 25D11 (20 μM), XL1-blue cells in white light for 60 min. (**E**) Effect of catalase on the bactericidal action of antibodies against *E. coli* XL1-blue [reported as percent recovered colony forming units (CFUs) at the start of the experiment ($t = 0$ min)]. Each group was irradiated with white light for 60 min at 4°C. The bacterial cell density was ~ 10^7 cells/ml in PBS The experimental groups (1 to 7) were treated were as follows. Group 1: *E. coli* XL1-blue and HPIX. Group 2: *E. coli* XL1-blue and nonspecific murine monoclonal antibody 84G3 (20 μM). Group 3: *E. coli* XL1-blue HPIX and 84G3 (20 μM). Group 4: *E. coli* XL1-blue HPIX, 84G3 (20 μM) and catalase (13mU/ml). Group 5: *E. coli* XL1-blue and specific rabbit polyclonal antibody (20 μM). Group 6: *E. coli* XL1-blue HPIX) and specific rabbit polyclonal antibody (20 μM). Group 7: *E. coli* XL1-blue, HPIX, specific rabbit polyclonal antibody (20 μM) and catalase (13mU/ml). Each point is reported as the mean value ± S.E.M. of multiple experiments ($n = 6$). **Denotes a *P* value < 0.01 relative to controls at the same time point. No
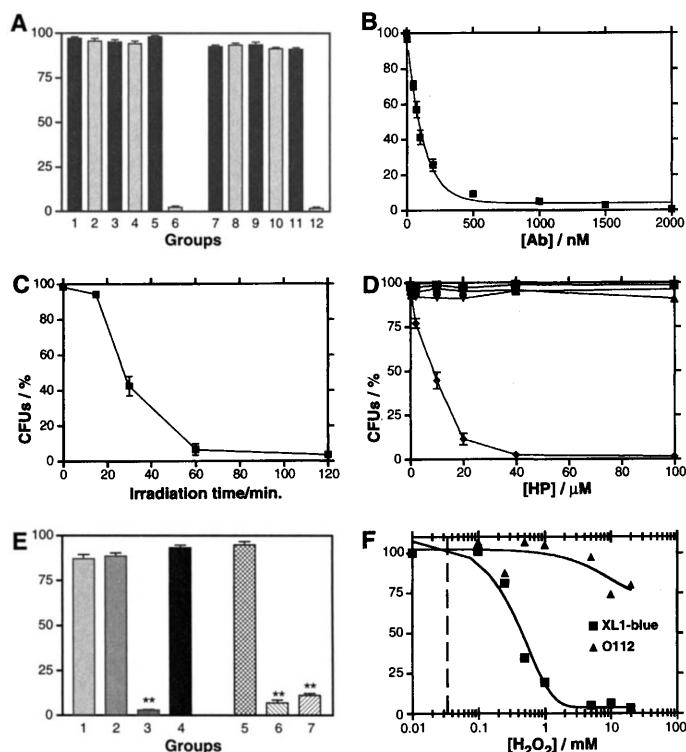
bactericidal activity was observed in any of the dark controls (data not shown) (**F**) Concentration-dependent toxicity of H_2O_2 on the viability of *E. coli* XL1-blue and O112a,c serotypes. The vertical hatched line is the concentration of H_2O_2 expected to be generated by antibodies during a 60 min incubation using the conditions described in Fig. 1 and (*18*). The value of 35 ± 5 μM H_2O_2 is the mean value determined from 12 different monoclonal antibodies from at least duplicate measurements.
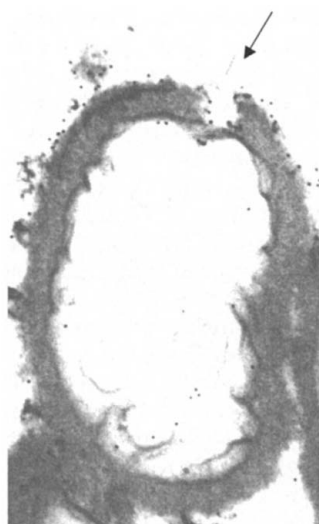

Fig. 2. *E. coli* O112a,c cell after exposure to antigen-specific murine monoclonal IgG (15404, 20 μM), HPIX in PBS and visible light for 1 hour at 4°C (<5% viable). To visualize the sites of antibody attachment gold-labeled goat anti-mouse antibodies were added after completion of the bactericidal assay (*6*). The arrow points to a puncture in the cell and plasma membrane.

vations support the key role of both $^1O_2^*$ and the water-oxidation pathway of antibodies in this bactericidal activity.

Given that H_2O_2 is the ultimate product of the antibody-catalyzed water-oxidation pathway (*3, 5*), we reasoned that this was the principal killing agent observed in our assays. Consistent with this notion, catalase completely protected against the bactericidal activity of nonspecific antibodies (Fig. 1E) (*10*). However, quantification of H_2O_2 toxicity on the two *E. coli* cell lines revealed that levels of H_2O_2 generated by nonspecific antibodies (35 ± 5 μM) were between 1 and 4 orders of magnitude below that required to kill 50% of the bacteria (Fig. 1F) (*6, 11*).

Gold-labeled secondary antibodies and electron microscopy were used to correlate the morphological damage to sites on the bacterial cell wall where antibodies were bound (*6*). In the bactericidal pathway, there are clear stages in which oxidative damage leads to an increased permeability of the cell wall and plasma membrane to water where killing is associated with the production of holes in the bacterial cell wall at the sites of antigen-antibody union (Fig. 2). The observed morphologies induced by antibody-mediated killing are similar to those seen when bacteria are destroyed by phagocytic cells (*12*).
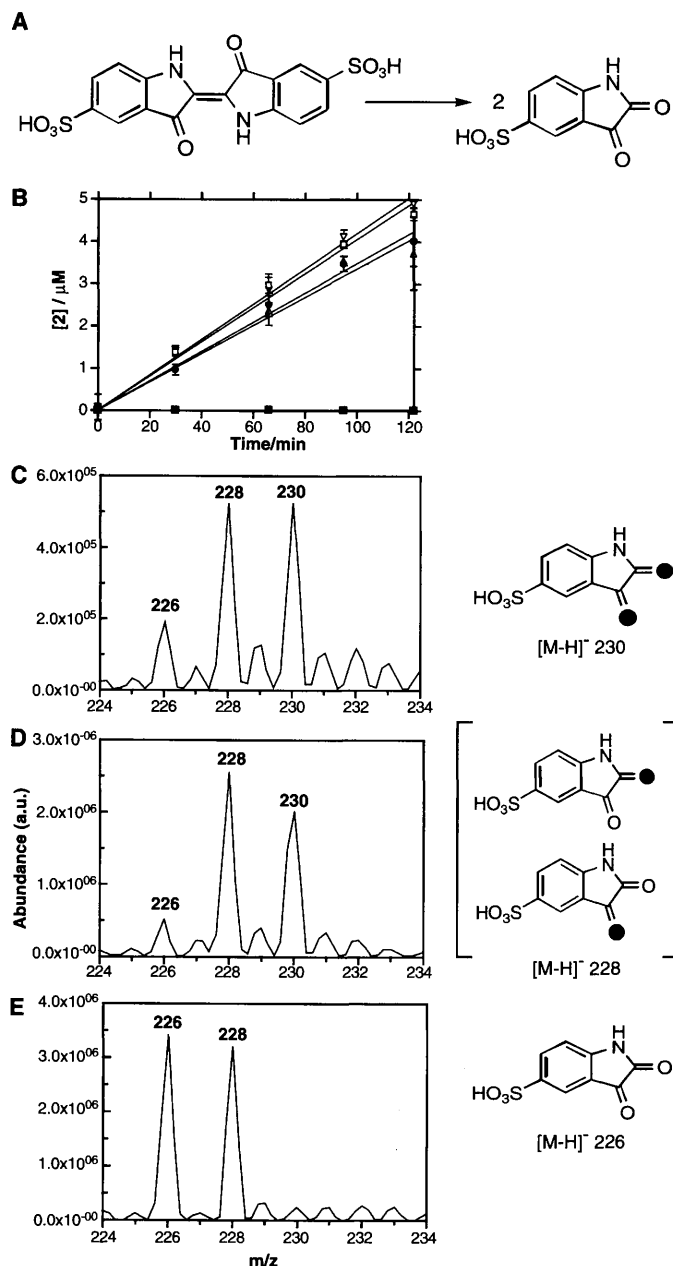
The finding that the toxicity of H_2O_2 to *E. coli* was below that generated by antibodies

forced us to re-examine the implication of the experiments with catalase, discussed above. H_2O_2 could potentially react with some other chemical species also generated by the antibody to produce the bactericidal molecule(s). Thus, by destroying H_2O_2, catalase prevents the formation of these species. Alternatively, other species formed on the way to H_2O_2 may also be substrates for catalase. In the course of exploring which bactericidal agents might contribute to H_2O_2-mediated killing, we observed that one of the antibody-generated oxidants possesses the chemical signature of ozone (O_3).

Theoretical calculations have shown that ozone is a plausible intermediate that could be produced during the water-oxidation pathway (*13*). Although ozone itself is highly bactericidal, there also exists a reaction between H_2O_2 and O_3 that is termed the peroxone process. This process is exploited at the industrial scale for water purification, where it has been reported that a combination of H_2O_2 and O_3 is far more toxic to bacteria than either alone (*14, 15*).

Under the aqueous conditions used in our assays, ozone is quite long lived [half-life ($t_{1/2}$) = 66 s] (*6*). Therefore, we began a search for O_3 production during the water-oxidation pathway by antibodies using indigo

Fig. 3. (A) Oxidation reaction of indigo carmine **1** to isatin sulfonic acid **2**. (B) Progress of isatin sulfonic acid **2** production from indigo carmine **1** (1 mM) during UV irradiation (312 nm, 0.8 mW cm^{-2}) of antibodies in PBS in the presence and absence of catalase (6). Each point is reported as the mean ± SEM. of at least duplicate determinations. Linear regression analysis was performed with Graphpad Prism v.3.0 software; v = rate of formation of **2**. (▽), Sheep polyclonal IgG (20 μM) v = 34.8 ± 1.8 nM/min; (□); murine monoclonal antibody 33F12 (20 μM) v = 40.5 ± 1.5 nm/min; (●); sheep polyclonal IgG (20 μM) and soluble catalase (13 mU/ml) v = 33.5 ± 2.3 nM/min; (■), murine monoclonal antibody 33F12 (20 μM) and soluble catalase (13 mU/ml) v = 41.8 ± 1.2 nM/min. (C to E) Electrospray ionization (negative polarity) mass spectra of isatin sulfonic acid **2** [(M-H)$^-$ 226, (M-H)$^-$ 228 (^{18}O), and (M-H)$^-$ (2 x ^{18}O)] produced during the oxidation of indigo carmine **1** (1 mM) in H$_2$^{18}O (> 95% ^{18}O) phosphate buffer (PB, 100 mM) at room temperature under conditions as follows: (C) Conventional ozonolysis (600 μM in PB) for 5 min. (D) Irradiation of HPIX with white light and sheep polyclonal IgG (20 μM) with white light for 4 hours. (E) Irradiation of HPIX with white light for 4 hours.

carmine **1**, a sensitive probe for O$_3$ detection in aqueous systems (16, 17). Conventional ozonolysis of **1** in aqueous solution leads to bleaching of the characteristic absorbance of **1** (λ_{max} = 610 nm; ε = 20,000 M^{-1}cm^{-1}) and the formation of isatin sulfonic acid **2** (Fig. 3A).

When antibody solutions in PBS were irradiated with ultraviolet (UV) light, under conditions where the water-oxidation pathway was functioning, in the presence of **1** (1 mM), catalase-independent bleaching of **1** and formation of **2** was observed. (6) (Fig. 3B). The initial rate of antibody-mediated conversion of **1** into **2** was linear, independent of the antibody preparation [sheep polyclonal immunoglobulin G (IgG) = 34.8 ±

1.8 nM min^{-1}; 33F12 = 40.5 ± 1.5 nM min^{-1}] and equivalent to 12% of H$_2$O$_2$ formation (3).

Though the oxidative cleavage of the C–C double bond of indigocarmine **1** is a sensitive probe for ozone detection, it is not a specific one. We have confirmed that ^{1}O$_2$* also bleaches solutions of **1** to form **2** by oxidative double-bond cleavage (6). Given that ^{1}O$_2$* is generated by antibodies upon UV irradiation (3, 5), we sought a means of analytically differentiating between oxidative cleavage of **1** to **2** by ^{1}O$_2$* as opposed to one cleaved by O$_3$. We observed that cleavage by O$_3$ can be distinguished from cleavage by ^{1}O$_2$* through the different behavior of these two oxidation processes by observing ^{18}O incorporation

from the reaction solvent H$_2$^{18}O into the cleavage product **2** (18). Experimentally, conventional ozonolysis of **1** in phosphate buffer (10 mM, prepared with H$_2$^{18}O) leads to the mass peak [M-H]$^-$ 230 for **2** being obtained (Fig. 3D), a result of exchange of ^{18}O of water into the amide carbonyl of **2** during the oxidation process. This mass fragment is not detected when **1** is oxidized by ^{1}O$_2$* (Fig. 3E) (19, 20). However, when sheep IgG (20 μM) and HPIX were irradiated with visible light (2.8 mW cm^{-2}) in the presence of **1**, oxidized product **2** was formed that possesses the mass peak [M-H]$^-$230, suggesting that an oxidant with the chemical signature of ozone was among the reaction intermediates formed along the antibody-mediated water oxidation pathway (Fig. 3C).

Given the importance of the claim that ozone may be being generated during this process, we sought to further substantiate this observation with a chemical probe that contains a normal carbon-carbon double bond. The choice of the probes, 3- and 4-vinylbenzoic acid (**3** and **4**, respectively), was guided by their aqueous solubility coupled with ease of detecting the putative reaction products 3- and 4-carboxybenzaldehyde (**5a**, and **5b**, respectively) and 3- and 4-oxiranylbenzoic acid (**6a** and **6b**, respectively) (fig. S3) by high-performance liquid chromatography (HPLC) (6, 21).

When a solution of sheep polyclonal antibody (20 μM) in PBS was irradiated with UV light (312 nm, 0.8 mW cm^{-2}), conditions where the water-oxidation pathway was activated in the presence of **3** and **4** (1 mM) formed the oxidation products 3-carboxybenzaldehyde **5a** and 3-oxiranyl benzoic acid **6a** (ratio 15:1, 1.5% conversion of **3** after 3 h) and 4-carboxybenzaldehyde **5b** and 4-oxiranyl-benzoic acid **6b** (ratio of 10:1, 2% conversion to **4** after 3 hours), respectively. These products are also observed when **3** and **4** are ozonolized in PBS in a conventional way (6). In sharp contrast, ^{1}O$_2$* generated by HPIX and visible light does not cause any detectable oxidation of either **3** or **4** under these conditions. These observations with the orthogonal ozone probes **3** and **4** directly parallel the experimental observations with indigo carmine **1** and add further support to the notion that an oxidant with the chemical signature of O$_3$ is generated during the antibody-catalyzed water-oxidation pathway.

Neutrophils are central to a host's defense against bacteria and have been shown to have antibodies on their cell surface (6, 22) and to have the ability, upon activation, to generate a cocktail of powerful oxidants that have been suggested to include ^{1}O$_2$* (23, 24). Thus, these cells may offer a nonphotochemical biological source of ^{1}O$_2$* that, with antibodies, might be capable of processing this substrate via the water-oxidation pathway.

Also, utilization of a cellular source of $^1O_2$ by antibodies offers a broader potential biological context for physiological conditions that go beyond those that require light activation.

After activation with phorbol myristate (1 µg/ml), human neutrophils (1.5 × 10⁷ cells/ml) produce an oxidant that cleaves indigo carmine 1 and generates isatin sulfonic acid 2 (Fig. 4A) (25–27). Between 40 and 50% of the possible yield of isatin sulfonic acid 2 (25.1 ± 0.3 µM of a potential 60 µM) from 1 occurs during the neutrophil cascade, revealing that a high concentration of this oxidant is generated during the oxidative pathway. When this same experiment is carried out with nuetrophils in $H_2{}^{18}O$ water, between 50 and 75% of the amide carbonyl oxygen of 2 incorporates ^{18}O, as shown by the intensity of the [M-H]⁻ 230 mass peak in the mass spectrum (MS) of the isolated cleaved product 2 (Fig. 4B). This ^{18}O incorporation with neutrophils parallels the observation with both conventional ozonolysis and antibody-mediated oxidative cleavage of 1. Work must continue in order to determine whether the formation of this oxidant with the chemical signature of ozone by neutrophils is solely due to the antibody-mediated water oxidation pathway, or whether neutrophils are also capable of forming this oxidant when activated.

To put these experiments into a physiological context, we studied an inflammatory model in vivo. The Arthus reaction is the

classical inflammatory response that occurs when antigen-antibody union occurs in a tissue (28). In an immunologically competent host, antigen-antibody union activates complement, thereby initiating an inflammatory

cascade, which includes the release of chemokines and granulocyte migration to the site where the immune complexes are formed.

A reversed passive Arthus reaction was generated in the skin of Sprague-Dawley rats using a bovine serum albumin (BSA)–antibody to BSA system (6). The inflammatory response at the site of antibody-antigen union peaked at approximately 8 hours and was associated with the classical gross and histological features of an Arthus reaction. Analytical studies were carried out on punch biopsies of either the inflammatory lesion or control skin samples from adjacent sites. These tissue samples were rapidly isolated and homogenized in a solution of indigo carmine (200 µM) in either PBS or PBS containing >95% $H_2{}^{18}O$. Bleaching of the indigo carmine solution was observed in the inflammatory lesion but not with any control samples. The oxidation of 1 by the Arthus tissue was immediate and corresponded to ~10% of the starting concentration (20 µM) of 1, as determined by UV absorbance at 610 nm. HPLC analysis confirmed that the oxidation of 1 was accompanied by formation of 2 as occurred in the experiments with purified antibodies and isolated neutrophils (Fig. 5A). MS analysis of 2 formed by the Arthus biopsies that had been placed into $H_2{}^{18}O$-containing PBS revealed that the [M-H]⁻ 230 fragment was present, confirming that this inflammatory lesion contains an oxidant with the chemical signature of ozone (Fig. 5B).

The results presented here may be biologically important in terms of the role of the immune system in both defense and its counterpart, induction of disease. The discovery of the bactericidal activity of antibodies in the presence of $^1O_2{}^*$ is the first direct evidence that they can destroy their antigenic targets in the absence of complement or phagocytes. Further, our study demonstrates that a molecule, which appears to be ozone, is generated by antibodies during bacterial killing by activated neutrophils and in an inflammatory response in vivo. However, production of other short-lived trioxygen adducts that might have the same chemical signature as ozone cannot be discounted, although, as with ozone, evidence for the generation of such oxidants would be new to biology.

Ozone is a highly toxic, but short-lived substance. These properties would make it an ideal effector molecule, because any damage would be localized to the site of inflammation. Like other immune effectors, its synthesis in the systems studied here was triggered by antigen-antibody union that, in this case, occurs when activated neutrophils at the site of an infection generate $^1O_2{}^*$, which is the substrate for the antibody-catalyzed water-oxidation process. Ozone shares another key hallmark of immune effectors in that it not only kills but also functions as a signaling device that serves to amplify the inflamma-
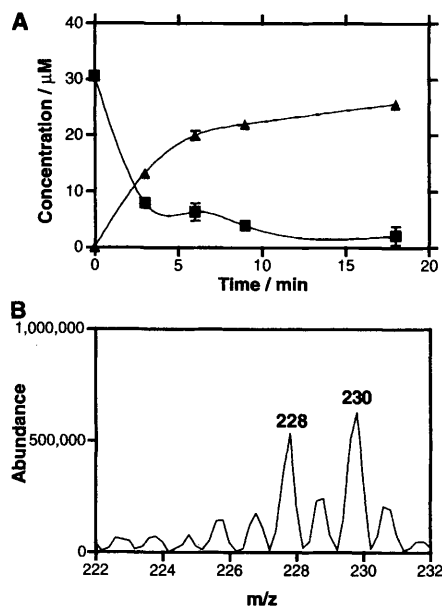

Fig. 4. (A) Oxidation of **1** (30 µM) (■) and formation of **2** (▲) by human neutrophils (PMNs) activated with phorbol myristate in PBS at 37°C. No oxidation of **1** occurs with PMNs that are not activated (data not shown). Neutrophils were prepared as previously described (25). (B) Negative-ion electrospray MS of the isatin sulfonic acid **2** produced during the oxidation of **1** by activated human neutrophils, under the conditions described in (A).
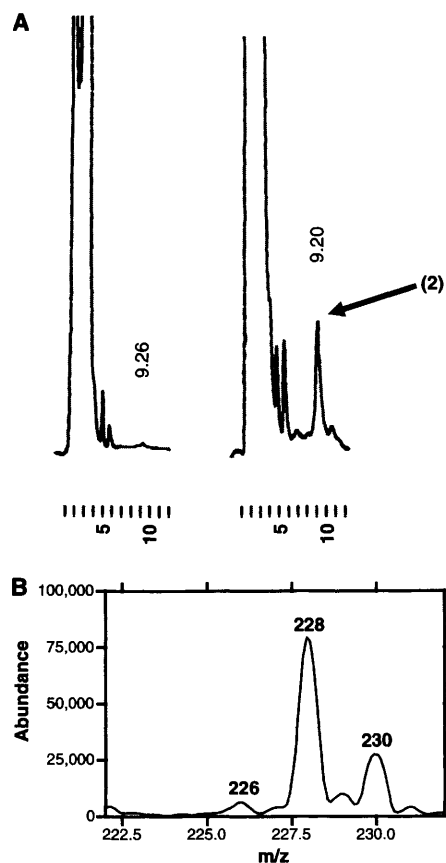

Fig. 5. Analytical evidence for the production of an oxidant with the chemical signature of ozone during the reversed passive Arthus reaction (6). A reversed passive Arthus was induced in Sprague-Dawley rats (150 to 200 g) by intravenous (i.v.) injection of BSA (100 µλ, 10 mg/ml) and a simultaneous intradermal injection of a polyclonal anti-BSA IgG (100 µl, 10 mg/ml). For control purposes, Sprague Dawley rats received an intradermal injection of a polyclonal non-BSA–specific IgG (100 µl, 10 mg/ml) preparation or PBS (100 µl) in adjacent skin sites. Eight hours after the i.v. administration of BSA (100 µλ, 10 mg/ml), the animal was then killed, and areas of injection were harvested using an 8-mm punch biopsy. Biopsy specimens from each reaction were added to a tissue homogenizer containing indigo carmine (50 µM). (A) HPLC traces of tissue homogenates generated from rat skin biopsies. The left trace is an analysis of the oxidation products of **1** generated from a control skin site that had been injected with PBS. The right trace was from an adjacent Arthus lesion generated by anti-BSA IgG. Note the presence of isatin sulfonic acid **2**, retention time R_T ~ 9.2 to 9.3 min. (B) Electrospray MS of the tissue homogenate obtained from an Arthus lesion, generated as detailed above, that had been added to a solution of indigo carmine (200 µM) in PBS containing > 95% $H_2{}^{18}O$.

tory response by the production of nuclear factor kappa B (NF-κB), interleukin-6 (IL-6), and tumor necrosis factor–α (TNF-α) (29, 30). Lastly, the catalytic antibody field has shown that antibodies are capable of much more complex chemistry than simple binding. It has not been previously thought that this potential for complex chemistry plays a role in their in vivo function. However, in light of our data, one must now consider that all antibodies have an innate catalytic potential that may be exploited for host protection.

References and Notes
1. R. B. Sim, K. B. Reid, *Immunol. Today* **12**, 307 (1991)
2. P. Wentworth Jr., *Science* **296**, 2247 (2002).
3. A. D. Wentworth, L. H. Jones, P. Wentworth Jr., K. D. Janda, R. A. Lerner *Proc. Natl. Acad. Sci. U.S.A.* **97**, 10930 (2000).
4. S. J. Klebanoff, in *Enclycopedia of Immunology*, P. J. Delves, I. M. Roitt, Eds. (Academic Press, San Diego, 1998), pp. 1713–1718.
5. P. Wentworth Jr. *et al.*, *Science* **293**, 1806 (2001).
6. Materials and Methods available as supporting online material (SOM) on *Science* Online.
7. F. Berthiaume *et al.*, *Biotechnology* **12**, 703 (1994).
8. The only requirement for initiation of H_2O_2 production by antibodies is exposure to the substrate $^1O_2^*$ (3). Antibodies can utilize $^1O_2^*$ generated by endogenous or exogenous photochemical sources, using UV or white light or chemical sources such as anthracene-9,10-dipropionic acid endoperoxide. Therefore, the choice of a $^1O_2^*$-generating system is guided solely by experimental considerations such as reaction efficiency and cellular or substrate sensitivity to irradiation.
9. F. Wilkinson, W. P. Helman, A. B. Ross, *J. Phys. Chem. Ref. Data* **22**, 113 (1993).
10. An analysis of the effects of additives, such as catalase, on intermediates that are generated during the water-oxidation pathway is only meaningful with antigen nonspecific antibodies because they are not encumbered by the sequestration and proximity effects of antigen-specific antibodies. The fact that the effect of catalase is not as dramatic on the bactericidal effects when antibodies specific for bacterial surface antigens are used is consistent with this reasoning.
11. The issue of proximity makes a stoichiometric comparison between the effects of H_2O_2 in solution and H_2O_2 generated on the bacterial cell surface complicated in the case of antigen-specific antibodies. Therefore, antibody-generated H_2O_2 and H_2O_2 in solution were compared with antigen nonspecific antibodies.
12. P. Hofman *et al.*, *Infect. Immun.* **68**, 449 (2000).
13. X. Xu, R. P. Muller, W. A. Goddard III, *Proc. Natl. Acad. Sci. U.S.A.* **99**, 3376 (2002).
14. W. H. Glaze, J. W. Kang, D. H. Chapin, *Ozone Sci. Eng.* **8**, 335 (1987).
15. C.-H. Kuo, L. Zhong, M. E. Zappi, A. P. Hong, *Can. J. Chem. Eng.* **77**, 473 (1999).
16. K. Takeuchi, I. Takeuchi, *Anal. Chem.* **61**, 619 (1989).
17. K. Takeuchi, S. Kutsuna, T. Ibusuki, *Anal. Chim. Acta* **230**, 183 (1990).
18. All ^{18}O isotope incorporations experiments were carried out using HPIX and white light, because the $^1O_2^*$ source because preliminary studies had revealed that rapid and reversible exchange of the oxygen in the amide carbonyl of **2** with water occurred in the presence of UV light (312 nm; 0.8 μW cm^{-2}). In white light, however no discernable exchange occurs during the experiment.
19. We presume that ozonolysis leads to ^{18}O isotope incorporation into the lactam carbonyl of **2** by trapping the presumed carbonyl oxide intermediate generated during ozonolysis by $H_2{}^{18}O$. We attribute the lack of isotope incorporation into **2** after oxidation by $^1O_2^*$ in phosphate buffer (PB) as being in accord with the known propensity of alkenes that contain no allylic hydrogens and at least one electron-donating atom α-to the olefin to form dioxetane intermedi-
ates which collapse to further products via a presumed retro [2+2] process (20).
20. A. A. Gorman, M. A. J. Rodgers, *Chem. Soc. Rev.* **10**, 205 (1981).
21. Vinyl benzoic acids **3** and **4** and their oxidized derivatives **5a** and **-b** and **6a** and **-b** used during these experiments are shown in the SOM (6).
22. E. L. Alexander, J. A. Titus, D. M. Segal, *J. Immunol. Methods* **22**, 263 (1978).
23. M. J. Steinbeck, A. U. Khan, M. J. Karnovsky, *J. Biol. Chem.* **267**, 13425 (1992).
24. ———, *J. Biol. Chem.* **268**, 15649 (1993).
25. Human neutrophils were prepared as previously described (26).
26. M. Markert, P. C. Andrews, B. M. Babior, *Methods Enzymol.* **105**, 358 (1984).
27. Hypochlorous acid (HOCl) is an oxidant known to be produced by neutrophils. In our experiments, NaOCl (2 mM) in PBS oxidizes **1** (100 μM) but does not cleave the double bond of **1** to yield isatin sulfonic acid **2** (6).
28. J. Kohl, J. E. Gessner *Mol. Immunol.* **36**, 893 (2002).
29. G. F. Joos *et al.*, *Allergy* **55**, 321 (2000).
30. H.-Y. Cho *et al.*, *Am. J. Physiol.* **280**, L537 (2002).
31. We thank members of the TSRI mass-spectroscopy facility, especially G. Suizdak and M. Sonderegger for assistance with the isotope analysis, M. Wood for expert assistance with the electron microscopy experiments, and C. Cochran for supply of the antibody to BSA. Supported by NIH GM43858 (K.D.J.), PO1CA27489 (Program Project Grant to K.D.J. and R.A.L.) and The Skaggs Institute for Chemical Biology. J.E.M. is an Achievement Rewards for College Scientists (ARCS) Foundation graduate fellow; C.T. is supported in part by NIH training grant (5T32AI07606).

Maintenance of Serological Memory by Polyclonal Activation of Human Memory B Cells

Nadia L. Bernasconi,* Elisabetta Traggiai,* Antonio Lanzavecchia†

Production of antibodies can last for a lifetime, through mechanisms that remain poorly understood. Here, we show that human memory B lymphocytes proliferate and differentiate into plasma cells in response to polyclonal stimuli, such as bystander T cell help and CpG DNA. Furthermore, plasma cells secreting antibodies to recall antigens are produced in vivo at levels proportional to the frequency of specific memory B cells, even several years after antigenic stimulation. Although antigen boosting leads to a transient increase in specific antibody levels, ongoing polyclonal activation of memory B cells offers a means to maintain serological memory for a human lifetime.

Stimulation by antigen through the B cell receptor (BCR) followed by cognate T cell help drives proliferation and differentiation of antigen-specific naïve B lymphocytes into memory B cells and plasma cells (1, 2). Memory B cells carrying somatically mutated immunoglobulin (Ig) genes survive in secondary lymphoid organs in the absence of antigen (3) and mediate secondary immune responses upon rechallenge. In contrast, plasma cells are terminally differentiated, nondividing cells that home to spleen and bone marrow and are the main source of antibody, which they secrete at a high rate. Mouse plasma cells can be long-lived and are able to sustain antibody production for several months in the absence of memory B cells or antigen (4, 5). However, it is less likely that long-lived plasma cells produced during an immune response will maintain a constant supply of specific antibody over a human

life-span, because even long-lived plasma cells would eventually need to be replenished over a human lifetime.

Whether persisting antigen is required to maintain serological memory remains debated (6–8). Antigen-driven proliferation and differentiation of memory B cell to short-lived plasma cells induces high levels of protective antibodies (9). Yet, if persistence of antigen was the only mechanism available to maintain antibody production, immunological memory would be limited to persisting antigens. We therefore searched for alternative mechanisms that might ensure sustained proliferation and differentiation of memory B cells, independently of persisting antigen.

Two types of polyclonal stimuli exist that can trigger B lymphocyte proliferation and differentiation in the absence of antigen: (i) those derived from microbial products, such as lipopolysaccharide or unmethylated single-stranded DNA motifs (CpG oligonucleotides), which stimulate B cells via TLR4 (Toll-like receptor 4) and TLR9, respectively (10, 11); and (ii) T cells activated by a third-party antigen, which stimulate B cells in a noncognate fashion via CD40 ligand and cy-

Institute for Research in Biomedicine, Via Vela 6, CH 6500 Bellinzona, Switzerland.

*These authors contributed equally to this work.
†To whom correspondence should be addressed. E-mail: lanzavecchia@irb.unisi.ch